Eur. Phys. J. D **9**, 263–267 (1999)

THE EUROPEAN PHYSICAL JOURNAL D
EDP Sciences

Photoelectron spectra of small LaO_n^- clusters: decreasing electron affinity upon increasing the number of oxygen atoms

R. Klingeler, G. Lüttgens, N. Pontius, R. Rochow, P.S. Bechthold, M. Neeb, and W. Eberhardt

Forschungszentrum Jülich GmbH, Institut für Festkörperforschung, D-52425 Jülich, Germany

Received: 2 September 1998 / Received in final form: 27 October 1998

Abstract. We present mass selected photoelectron spectra of small lanthanum oxide cluster anions LaO_n^- ($n = 1 - 5$) which have been generated in a laser vaporization cluster source. The electron affinity of the lanthanum oxide clusters drops continuously with the number of chemisorbed oxygen atoms as revealed from the anion photoelectron spectra. The decreasing electron affinity behaves contrary to several other metal oxide clusters. The geometry of some of the measured clusters are discussed in comparsion with configuration interaction and density functional calculations using a Gaussian94 program package.

PACS. 33.60.Cv Ultraviolet and vacuum ultraviolet photoelectron spectra – 33.80.Eh Autoionization, photoionization and photodetachment – 36.40.Mr Spectroscopy and geometrical structure of clusters

The work function of several metals can effectively be lowered by covering the surface with a thin layer of mono- or divalent metaloxides. This phenomenon is technologically used to enhance the electron yield of thermal cathodes. The oxides of barium and caesium are effective materials to lower the work function. Lanthanum is placed right next to barium and caesium in the periodic table. The work function of solid lanthanum oxide (La_2O_3) is 2.8 eV. Small lanthanum oxide clusters have a considerably lower electron affinity than the bulk material as revealed in the present manuscript. Furthermore the electron affinity, which corresponds to the work function of a solid, becomes reduced with an increase of the number of O atoms. This is in contrast to several other metal oxide clusters for which the electron affinity increases with the number of chemisorbed oxygen atoms as has recently been shown for small iron-, titanium-, and aluminum oxide clusters [1–3].

The lanthanum oxide anions have been generated in a pulsed laser vaporization plasma source. After an adiabatic expansion the cluster anions are accelerated and focused by a Wiley-McLaren ion optic. The anions are mass selected by their time of flight prior to the detachment process. Electrons are detached by a Q-switched Nd:YAG laser pulse (3.495 eV). The kinetic energy of the emitted electrons is analyzed in a magnetic-bottle time-of-flight analyzer [4].

Density functional (DF) and single excitation configuration interaction (CI) calculations have been performed using a Gaussian94 program package [5]. Both type of calculations have been excecuted with the LanL2DZ basis set under inclusion of additional d- and f-wave functions. Using the Lee/Yang/Parr correlation functional [5] we found the results of the three parameter hybrid method of Becke [5] in good agreement with former experimental results on LaO. Xα exchange [5] has been applied to determine the charge transfer and bond length of the clusters. The photoelectron spectra are compared to the excited states of the neutral cluster. The CI calculations have been performed in the relaxed geometry of the neutral.

Figure 1 shows the photoelectron spectra of small LaO_n^- clusters ($n = 1 - 4$) as directly obtained from a pure lanthanum rod.

The photoelectron spectrum of LaO^- is shown in Fig. 1a. The electron affinity is 0.97 ± 0.10 eV as taken from the onset of the first peak. The ground state electron configuration of LaO is $(1\sigma)^2(2\sigma)^2(1\pi)^4(3\sigma)^1(1\delta)^0(2\pi)^0(4\sigma)^0(^2\Sigma)$ [6]. The empty states are derived from the La5d orbitals which split under the influence of the oxygen ligand field into the 1δ, 2π and 4σ orbitals, respectively. The second and third photoelectron peak at 1.8 and 2.6 eV correspond to transitions from LaO^- to the excited states $^2\Delta$ and $^2\Pi$ which corresponds to the single particle electron configuration $(1\pi)^4(3\sigma)^0(1\delta)^1$ and $(1\pi)^4(3\sigma)^0(1\delta)^0(2\pi)^1$, respectively. The latter results from an electron transition into the LUMO+1. The 1δ-LUMO is purely La5d-derived. The LUMO+1 (2π) and LUMO+2 (4σ) states are reached via shake up transitions during the detachment process of the anion. The extra electron of the anion is most likely placed in the 3σ orbital yielding a $^1\Sigma$ ground state for LaO^-.

The overall peak structure in the photodetachment spectrum of LaO^- corresponds well to the optical absorption peaks of LaO [7] which is shown as bar diagram in Fig. 1a. The lower bars correspond to vibrational levels of the respective electronic states. The peak at 3.1 eV binding energy, not seen in the absorption spectrum, is assigned to a transition into a quartet final state (enlarged in Fig. 1a). Such quartet states have been predicted in the region be-

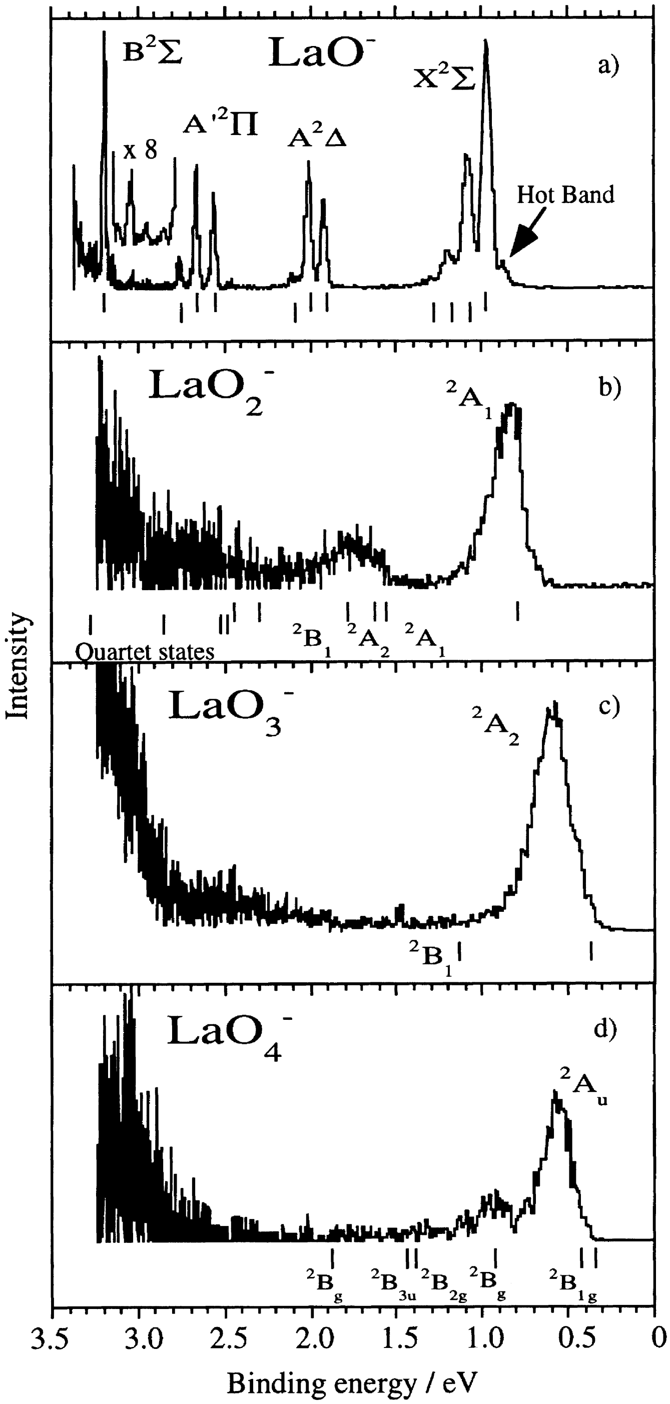

Fig. 1. Photoelectron spectra of LaO_n^- $(n = 1-4)$ at 3.49 eV photon energy. The clusters have been obtained with a pure He carrier gas. The PES of LaO^- agrees with the excitation energies of neutral LaO. The optical excitation energies are shown as vertical lines in (a). The line spectra in (b)–(d) represent the results of CI calculations relative to the measured electron affinity of LaO_2, LaO_3 and LaO_4.

tween the $A^2\Pi$ and $B^2\Sigma$ [6] final state transitions and are not detected in the optical absorption spectrum [7] due to the dipole selection rule $\Delta S = 0$. These low lying quartet states are a consequence of the odd number of valence electrons in LaO which gives rise to an open shell configuration in the neutral ground state. The spin-orbit coupling of the first ($^2\Delta$) and second excited state ($^2\Pi$) amounts to 88 and 103 meV, respectively. This is in agreement with the optical measurements in [7] which give a splitting of 87 and 107 meV, respectively. The vibrational frequency (887 cm^{-1}) of LaO is similar to that in the matrix isolated LaO molecule (813 cm^{-1}) [7].

A Mulliken population analysis yields a charge transfer from La to O of 0.5 $|e|$. The bonding in LaO is thus markedly covalent in which the O2$p\pi$ orbitals are effectively hybridized with the La5d orbitals and, moreover, slightly with the La4f orbitals.

Figure 1b shows the photoelectron spectrum of LaO_2^-. The peak at the lowest binding energy shows a broad envelope from 0.7–1.1 eV. The electron affinity is 0.79 eV. The shoulder on the low binding energy side of the peak is attributed to a hot-band. A second peak of LaO_2 is seen at 1.7 eV. The peak is less intense than the first peak but shows a comparable width. Two stable geometries have been calculated for LaO_2 in C_{2v} symmetry: One in which a central La-atom is bound to two O-atoms on either side of the La-atom and a second geometry in which an almost intact O_2 molecule is chemisorbed at one side of the La-atom. The photoelectron spectrum in Fig. 1b supports the existence of the latter isomer. In this geometry the two O-atoms are bound to each other and have the same distance to a laterally bound La-atom. Consequently, the bonding in LaO_2 can be visualized in terms of a charge transfer from La into the valence orbitals of an adsorbed O_2 molecule. The first peak in the photoelectron spectrum at 0.8 eV corresponds to the ionization of the La6s orbital. Ionization of this orbital results in neutral LaO_2 with a singly occupied 6s orbital and a $^2A_1$ ground state. The La6s orbital represents the HOMO (a_1) which is only slightly disturbed by the oxygen orbitals. The width of the first peak is possibly due to vibrational excitation of the totally symmetric normal modes which have vibrational frequencies of 509 and 796 cm^{-1}, respectively. The second photoelectron peak at 1.7 eV binding energy is associated with shake up transitions from the 6s orbital into the LUMO, LUMO+1 and LUMO+2, respectively. The energies of the shake up transitions correspond to the region of the second peak and are indicated by the upper bar diagram in Fig. 1b. Above 2.5 eV several transitions into quartet final states have been calculated.

The HOMO-1 and HOMO-2 in LaO_2 are derived from the twofold degenerate $1\pi_g$ orbital of O_2 which in C_{2v} symmetry splits into an a_2 and b_2 orbital, respectively (Fig. 2). A Mulliken population analysis gives a charge transfer of 0.5 $|e|$ from La6s into the $1\pi_g$ orbital of O_2 (Fig. 2). Due to the antibonding character of the $1\pi_g$ orbital the charge transfer leads to a prolongation of the O_2 bond length which correspondingly lowers the vibrational frequency. DF calculations reveal a vibrational frequency of the O−O bond of 796 cm^{-1} which is – as expected – distinctly lower than the of free O_2 (1580 cm^{-1}) [7].

The photoelectron spectrum of LaO_3^- is shown in Fig. 1c. The transition from the anionic ground state into the neutral is located at a binding energy of 0.5 eV. The

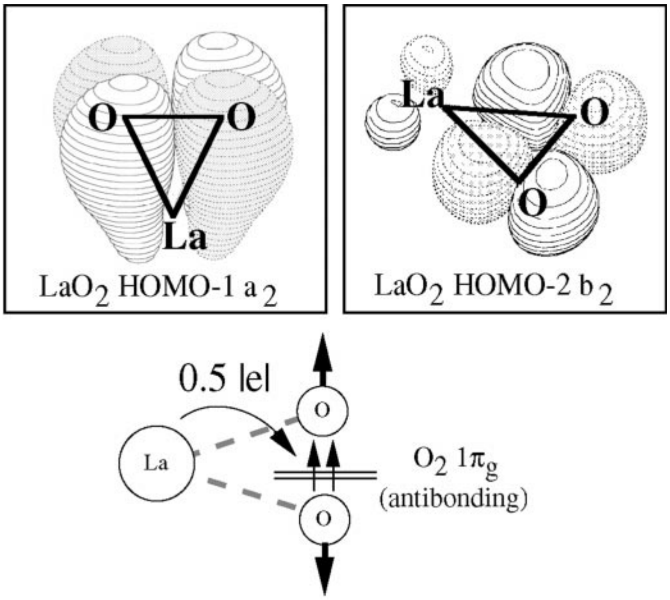

Fig. 2. Charge transfer model for the side-bonded C_{2v} species of LaO_2. An O_2 molecule is laterally adsorbed to a La-atom. Charge is transfered from La to the antibonding $1\pi_g$ orbital of O_2 which in turn leads to an increase of the O−O bond length with respect to free O_2.

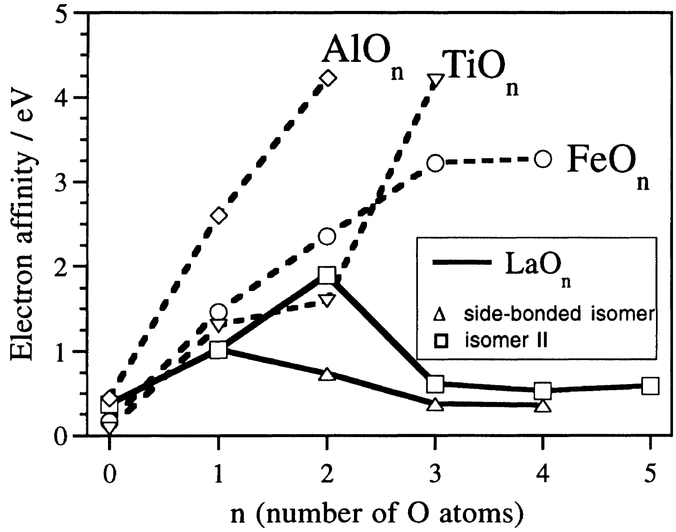

Fig. 3. Electron affinities of small metal oxide clusters (MeO_n) as a function of the number of O atoms. While the oxides of Fe, Al and Ti [1–3] show increasing electron affinities, these of the La oxide clusters decrease.

adiabatic electron affinity amounts to ~ 0.3 eV as revealed from a linear approximation of the low binding energy side of the first peak onto the energy axis. The width of the feature is due to vibrational broadening. Additionally, a small feature is seen at 2.5 eV which merges into a rising edge at the end of the spectrum. The geometry of LaO_3 is assembled from a LaO_2 molecule with an additional O-atom on the opposite side of the O_2 species. The point group is C_{2v} and the ground state of the neutral is $^2A_2$. The HOMO is a b_2 orbital which is derived from the $1\pi_g$ orbital of O_2 in contrast to the HOMO of LaO_2 which is primarily a La6*s* orbital. The electron configuration is $(a_2)^1(b_2)^2(b_1)^2(a_1)^2(b_2)^2(a_1)^0$. The LUMO ($a_1$) has primarily La-character. Note that the unpaired electron does not occupy the HOMO but a deeper a_2 orbital which is derived from the degenerate $1\pi_g$ O_2-orbital. The O−O bond length in LaO_3 is almost identical to O_2^- which suggests a considerable charge transfer from La into the antibonding $1\pi_g$ orbital of O_2. A Mulliken analysis predicts a total charge transfer of $\sim 1|e|$ of which $0.5|e|$ is located in the $1\pi_g-$ derived orbitals of O_2, like in LaO_2, and $0.5|e|$ in a 2*p*-orbital of the single O atom.

The spectrum of LaO_4^- shows a broad feature at 0.57 eV from which an adiabatic electron affinity of 0.35 eV is approximated (Fig. 1d). The electron affinity is almost equal to that of LaO_3. A second peak is seen at 0.94 eV which is interpreted as the transition from the anionic ground state into an electronically excited state of neutral LaO_4. Several transitions into higher excited states are indicated by small features between 1.3 and 2 eV. The peaks in Fig. 1d fit reasonably well to the excited states of a planar LaO_4 cluster with two O_2 units on either side of a La inversion center (D_{2h}).

The HOMO in LaO_4 is of b_{2u} symmetry mainly composed from a O2$p\pi$ molecular orbital. It is hybridized by $\sim 9\%$ with the La5$p\pi$ orbital. The O−O bond length is distinctly enlarged with respect to neutral O_2 which again demonstrates a charge transfer from the La-atom into the antibonding orbitals of the adsorbed O_2 molecules. A total charge transfer of $1.24|e|$ has been calculated. Within the D_{2h} point group the first peak in Fig. 1d corresponds to the transition into the ^2A_u ground state of LaO_4. The first excited state is a B_{1g} state which is almost degenerated with the ground state transition. The peak at 0.94 eV corresponds to the transition into the second excited state of LaO_4 (^2B_g). Between 1.3 and 2 eV several states with B symmetry have been calculated.

The electron affinities of the LaO_n clusters as a function of the number of oxygen atoms are displayed in Fig. 3 together with the corresponding values of other metal oxides. All the monoxides show an increase of the electron affinity with respect to the pure metal atom. This is most likely caused by the electronegativity of the oxygen atom which considerably lowers the electron density at the metal atom. The reduced charge density at the metal atom is responsible for the increase of the electron affinity since the HOMO in all the monoxides is predominantly of metal character (La6*s*, Ti3*d*, Fe3*d*, Al3*s*). The higher oxides show a different behaviour: While the electron affinities of the AlO_n, FeO_n and TiO_n ($n \geq 2$) clusters [1–3] increase with the number of oxygen atoms those of the corresponding La-oxide clusters decrease.

As discussed above, the LaO_n ($n \geq 2$) clusters contain at least one O_2 molecular unit adsorbed to the La-atom. The half-filled HOMO is primarily of pure La or of pure O_2 character. The electron affinities should thus not deviate too much from those of the isolated species which have indeed quite low electron affinities. The electron affinity of La is 0.37 eV; the one of O_2 amounts to 0.45 eV. Up to LaO_2

the HOMO is of La6s character. The electron affinity is therefore expected to be higher than that of the pure La-atom due to the reduced charge density at the metal atom. However, from LaO_2 onwards the HOMO changes into an O_2 derived $1\pi_g$ orbital. At this point the electron affinity drops below the electron affinity of a free O_2 molecule due the antibonding character of the HOMO in LaO_3 and LaO_4.

The geometries of TiO_n, AlO_n and FeO_n ($n \geq 2$) [2, 3, 8] differ from those of the La-oxides. For the former metal oxides the O_2 molecule dissociates under the influence of the metal atom. In consequence, the oxygen atoms are individually bound to the metal. FeO_2 and TiO_2 are bent clusters with C_{2v} symmetry. AlO_2 is a linear molecule which possesses the largest electron affinity. Due to a (OTiO) bond angle of ca. 110 degrees a weak O$-$O bond is formed which is a possible reason for the observation that the electron affinity is smaller in TiO_2 than this of the linear AlO_2 and the less bent FeO_2 (142 degrees [9]) but still higher than this of the side-bonded LaO_2 cluster.

It is interesting to note that with varying source conditions different isomers of the La-oxide clusters can be generated. The photoelectron spectra in Fig. 4 have been taken with a He/O_2 gas mixture containing 0.8% O_2. The photoelectron spectrum of LaO_2^- is shown in Fig. 4a. Three strong peaks are seen above 1.9 eV. The small feature below 1.5 eV is still due to the side-bonded LaO_2 isomer. The predominant isomer, however, has an electron affinity of 1.9 eV which originates from a linear OLaO cluster ($D_{\infty h}$). The open shell ground state of the linear cluster is a $^2\Sigma_u$ state. Several other excited states have been calculated between 2.1 and 2.5 eV as well as between 2.8 and 3.5 eV. The feature between 2.7 and 3.1 eV hides a vibrational progression (see inset) with a vibrational energy of ca. 366 cm^{-1}. This value is close to the energy of the antisymmetric stretching mode of the linear species (423 cm^{-1}). As a result of DF calculations there is another stable isomer, a bent OLaO structure. However, its vibrational energies ($\nu_1 = 637$ cm^{-1}, $\nu_2 = 130$ cm^{-1}, $\nu_3 = 219$ cm^{-1}) differ clearly from the experimental value of 366 cm^{-1}. In fact the electron affinity of the linear isomer is definitely higher than that of the side-bonded LaO_2 cluster.

Similar results have been obtained for NiO_2 and CuO_2 [10, 11]. Both of them reveal a side-bonded (O_2) complex as well as a linear O(Ni/Cu)O structure. In both cases the linear structure has the higher electron affinity [10, 11]. The spectra of LaO_3 and LaO_4 are also different under the above source condition. A vibrational fine structure with an energy of 500 cm^{-1} is indicated for LaO_4^- on the photoelectron feature at 2.3 eV. The electron affinities are reduced with respect to LaO_2 (see Fig. 3) but are close to those of the corresponding isomers produced without external O_2 supply. The decrease of the electron affinity continues up to LaO_5.

In conclusion the photodetachment spectra of small lanthanum oxide cluster anions have been measured. The clusters were produced in a pulsed laser evaporation source with and without an external oxygen supply. The electron affinities of the La-oxides are found to be quite small and decrease as a function of the oxygen amount. The behaviour is in sharp contrast to the electron affinities of small Al-, Fe- and Ti-oxide clusters [1–3], and is explained by the non-dissociative attachment of an O_2-adsorbate to the La-atom. The geometries and electron configurations of the neutral clusters have been revealed with the

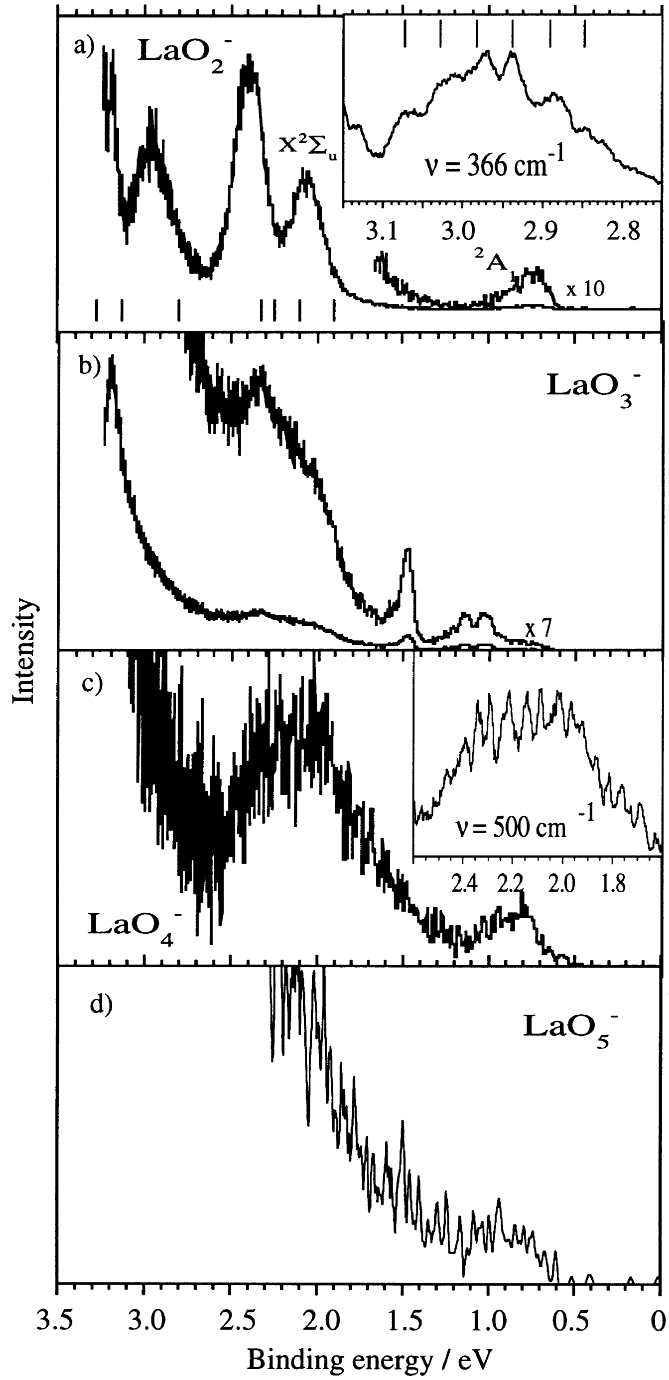

Fig. 4. Photoelectron spectra of LaO_n^- ($n = 2-5$) obtained with a He/O_2 carrier gas at 3.49 eV photon energy. The line spectrum in (a) shows the transition energies for a linear LaO_2 species ($D_{\infty h}$). The insets in (a) and (c) show vibrational fine structure revealed from a smooth fit.

aid based upon configuration interaction and density functional theory.

We are very grateful to L.-S. Wang for valuable dicussions during the prepartation of the manuscript. The work has been supported by the Sonderforschungsbereich SFB341 of the Deutsche Forschungsgemeinschaft.

References

1. L.-S. Wang, H. Wu, S.R. Desai: Phys. Rev. Lett. **76**, 4853 (1996)
2. H. Wu, L.-S. Wang: J. Chem. Phys. **107**, 8221 (1997)
3. S.R. Desai, H. Wu, C.M. Rohlfing, L.-S. Wang: J. Chem. Phys. **106**, 1309 (1997)
4. H. Handschuh, G. Ganteför, W. Eberhardt: Rev. Sci. Instrum. **66**, 3838 (1995)
5. M.J. Frisch, G.W. Trucks, H.B. Schlegel, P.M.W. Gill, B.G. Johnson, M.A. Robb, J.R. Cheeseman, T.A. Keith, G.A. Petersson, J.A. Montgomery, K. Raghavachari, M.A. Al-Laham, V.G. Zakrzewski, J.V. Ortiz, J.B. Foresman, J. Cioslowski, B.B. Stefanov, A. Nanayakkara, M. Challacombe, C.Y. Peng, P.Y. Ayala, W. Chen, M.W. Wong, J.L. Andres, E.S. Replogle, R. Gomperts, R.L. Martin, D.J. Fox, J.S. Binkley, D.J. Defrees, J. Baker, J.P. Steward, M. Head-Gordon, C. Gonzalez, J.A. Pople: Gaussian, Inc., Pittsburgh PA, 1995 and references therein
6. J. Schamps, M. Bencheikh, J.-C. Barthelat, R.W. Field: J. Chem. Phys. **103**, 8004 (1995)
7. K.P. Huber, G. Herzberg: *Molecular Spectra and Molecular Structure, IV Constants of Diatomic Molecules* (Van Nostrand Reinhold, New York 1979)
8. H. Wu, S.R. Desai, L.-S. Wang: J. Am. Chem. Soc. **118**, 5296 (1996)
9. L. Andrews, G.V. Chertihin, A. Ricca, C.W. Bauschlicher: J. Am. Chem. Soc. **118**, 467 (1996)
10. H. Wu, L.-S. Wang: J. Chem. Phys. **107**, 16 (1997)
11. H. Wu, S.R. Desai, L.-S. Wang: J. Phys. Chem. A **101**, 2103 (1997)